

1 **Identification of immunodominant linear epitopes from SARS-**
2 **CoV-2 patient plasma**

3

4 **Lluc Farrera-Soler¹, Jean-Pierre Daguer¹, Sofia Barluenga¹, Patrick Cohen², Sabrina**
5 **Pagano², Sabine Yerly², Laurent Kaiser^{2,3}, Nicolas Vuilleumier², Nicolas Winssinger^{1*}**

6

7 **1** Department of Organic Chemistry, NCCR Chemical Biology, Faculty of Science,
8 University of Geneva, Geneva, Switzerland.

9

10 **2** Division of Laboratory Medicine, Diagnostic Department, Geneva University Hospitals
11 and Faculty of Medicine, Geneva, Switzerland

12

13 **3** Division of Infectious Diseases, Geneva University Hospitals and Faculty of Medicine,
14 Geneva, Switzerland

15

16 * Corresponding author

17 E-mail: Nicolas.Winssinger@unige.ch

18 **Abstract**

19 A novel severe acute respiratory syndrome coronavirus (SARS-CoV-2) is the source of a
20 current pandemic (COVID-19) with devastating consequences in public health and
21 economic stability. Using a peptide array to map the antibody response of plasma
22 from healing patients, we identified immunodominant linear epitopes corresponding
23 to key proteolytic sites on the spike protein.

24

25 **Introduction**

26 On December 2019, a novel infectious disease causing pneumonia-like symptoms was
27 identified in the city of Wuhan in the province of Hubei (China) [1]. This new
28 coronavirus infectious disease (COVID-19) caused by the severe acute respiratory
29 syndrome coronavirus-2 (SARS-CoV-2) is having a devastating impact on public health
30 and economic stability on a global scale [2]. The World Health Organization declared it
31 a pandemic on the 11th March 2020.

32 Mapping the epitopes corresponding to the immune system's antibody response
33 against the virus is important for vaccine development [3, 4], diagnostic serological
34 tests [4] as well as for identifying neutralizing antibodies with therapeutic potential [5].
35 Indeed, epitope mapping of the SARS-CoV-1 revealed immunodominant epitopes and
36 identified neutralizing antibodies [6-13]. However, the observation of antibody-
37 dependent enhancement (ADE) of SARS-CoV-1 in non-human primates is concerning
38 and should be considered for vaccine development [14, 15]. While ADE mechanisms
39 arising from binding-only antibodies (non-neutralizing) are well documented, an ADE
40 mechanism with neutralizing antibodies for the related MERS-CoV was also

41 reported[16]. In this case, it was shown that neutralizing antibodies targeting the
42 receptor-binding domain (RBD) of the virus redirected viral entry to Fc-expressing cells,
43 broadening the host-targeted cells. Thus, antibodies generated by vaccination against
44 SARS-CoV-2 could enhance viral entry instead of offering protection, leading to
45 vaccine-associated enhanced respiratory disease (VARED) [17].

46 The homology between SARS-CoV-1 and SARS-CoV-2 rapidly led to the hypothesis
47 that neutralizing antibodies identified from patients in the SARS-CoV-1 in the 2003
48 epidemic could also be neutralizing SARS-CoV-2 [18, 19]. Other antibodies with
49 neutralizing activities have been discovered through different methodologies [20-25].
50 The rapid propagation of SARS-CoV-2 stimulated several studies predicting the
51 antigenic parts of the viral proteins *in silico* [26-32], and analyzing SARS-CoV-1
52 epitopes that were conserved in this new coronavirus [33-36]. More recently, the first
53 reports of experimental epitope mapping of the SARS-CoV-2 were deposited on
54 repositories [37-42].

55 Herein we report the preparation of a microarray to map the antibody response to
56 linear epitopes of the spike protein of SARS-CoV-2 and the analysis of 12 laboratory
57 confirmed COVID-19 cases and 6 negative controls using the described peptide
58 microarray.

59

60 **Materials and methods**

61 **Plasma specimens from COVID-19 and healthy patients.**

62 Anonymized leftovers of whole blood-EDTA were used for this method evaluation, in
63 accordance with our institution's ethical committee and national regulations. We
64 included 12 real-time RT-PCR confirmed COVID-19 cases hospitalized at the University

65 Hospitals of Geneva, and 6 unmatched negative blood samples from asymptomatic
66 donors, obtained during the same period (April 2020). Analyses (see below) were
67 performed within 72h of blood sampling without any freezing-thawing cycle.

68

69 **SARS-CoV-2 RT-PCR analyses and SARS-CoV-2 IgG serology**

70 As previously published [43], SARS-CoV-2 RT-PCR was performed according to
71 manufacturers' instructions on various platforms, including BD SARS-CoV-2 reagent kit
72 for BD Max system (Becton, Dickinson and Co, US) and Cobas 6800 SARS-CoV-2 RT-PCR
73 (Roche, Switzerland).

74 SARS-CoV-2 IgG serology against the S1-domain of the spike protein of SARS-CoV-2 was
75 assessed using the CE-marked Euroimmun IgG ELISA (Euroimmun AG, Lübeck,
76 Germany # EI 2606-9601 G). EDTA-plasma was diluted at 1:101 and assessed with the
77 IgG ELISA according to the manufacturer's instructions and has been extensively
78 reported elsewhere [43]. Median time from RT-PCR to serology testing was 3 weeks,
79 reason why sample were considered as healing rather than convalescent plasma. All
80 the 12 COVID-19 samples were considered as reactive against SARS-CoV-2.

81

82 **Synthesis of the peptide-PNA conjugate library.**

83 The library of peptide-PNA conjugate was synthesized by automated synthesis on an
84 Intavis peptide synthesizer as previously described [44, 45]. The synthesis was
85 initiated with the peptide followed by the PNA tag using a capping cycle after each
86 coupling. Hence, truncated peptides cannot hybridize on the microarray since they
87 will not have the necessary tag. A library of 200 linear peptides was constructed based
88 on the sequences of the spike ectodomain protein from SARS-CoV-2 (residues 1-1213-

89 Gene Bank: QHD43416.1), fragmenting the protein into two sets of 100 peptides
90 (12mer) with an overlap of 6 residues. Each peptide-PNA conjugate was positively
91 identified by MALDI analysis. See SI for full synthetic details and characterization data.

92

93 **Microarray epitope mapping.**

94 Microarrays were obtained from Agilent (Custom microarray slides, Agilent
95 ref:0309317100-100002). Each peptide-PNA is complementary to a DNA sequence
96 that is present 23 times at random positions on the array.

97 The arrays were incubated with plasma (1:150 dilution) for 1 hour at room
98 temperature, washed with PBS-T and dried by centrifugation prior to the next step.

99 The arrays were then incubated with Cy-3 labeled goat anti-human IgG (ab97170 from
100 Abcam, 1:500 dilution) for 30 min, washed with PBS-T and dried by centrifugation for
101 scanning. See SI for detailed procedures.

102 The fluorescence intensity on the array was measured on a GenePix 4100A
103 microarray scanner using the median value of fluorescent intensity. The data for each
104 peptide (23 spots) was plotted as a heat map of the median value from the 23 spots.
105 The high redundancy in the measurements and the use of a median function insures
106 that artifacts from a microarray experiment do not contribute to the consolidated
107 data.

108

109 **Validation of epitope 655-672.**

110 The peptide was synthesized according to the same protocol as for the library
111 synthesis, replacing the PNA tag with a biotin.

112 Fluorescent bead assay: 0.3 μ L of PierceTM High-Capacity Streptavidin Agarose
113 Beads (catalog n°: 20357 from Thermo ScientificTM) were mixed with 50 μ L of the
114 biotinylated peptide 10 μ M in PBS- T. The beads were incubated for 20 minutes and
115 thereafter blocked with 200 μ L of Fetal bovine serum for 10 minutes. The beads were
116 then washed once with 100 μ L PBS-T and 5 μ L of serum from either positive or
117 negative patients was added together with 450 μ L of PBS-T and 50 μ L of fetal bovine
118 serum in order to block unspecific interactions. The beads were then incubated for 90
119 minutes and subsequently washed 4 times with 100 μ L of PBS- T in order to remove all
120 the non-binders. Finally, 200 μ L of a 163nM solution of anti-human IgG-FITC (ab6854
121 from Abcam) in PBS-T with 0.5% BSA was added and incubated for 1 hour. The excess
122 of secondary antibody was washed away using 3 times 100 μ L of PBS-T and finally the
123 beads were imaged with a Leica SP8 inverted confocal microscope.

124 By Enzyme-Linked Immunosorbent Assay (ELISA): A solution of Streptavidin (ref:
125 S0677 from Sigma Aldrich), 100 μ L of an 80nM, in PBS was added to a Corning[®] 96-
126 well Clear Flat Bottom Polystyrene High Bind Microplate (catalog n°: 9018 from
127 Corning) and incubated overnight at 4°C. The plate was then washed three times with
128 300 μ L of PBS-T (60 seconds, room temperature) and 200 μ L of an 800nM solution of
129 biotinylated peptide in PBS-T was added and incubated for 90 minutes at 36°C. The
130 plate was then blocked with 300 μ L of PBS-T with 0.5% non-fat dry milk (60 minutes at
131 36°C). The plate was washed 3 times with 300 μ L of PBS-T (60 seconds, room
132 temperature) and a 1:300 diluted plasma in PBS-T-0.5% non-fat dry milk was added to
133 each well and incubated for 90 minutes at 36°C. After incubation of the plasma, the
134 plate was washed 3 times with 300 μ L PBS-T (60 seconds, room temperature), 1 time
135 with PBS-T 0.5% non-fat dry milk (60 minutes, 37°C) and again 3 times with 300 μ L

136 PBS-T (60 seconds, room temperature). 100 μ L of Goat Anti-Human-IgG HRP
137 conjugated (ab97175 from Abcam) 1:10000 diluted in PBS-T 0.5% BSA were added to
138 each well and incubated for 90 minutes at 37°C. The plate was then washed 3 times
139 with PBS-T (60 seconds, room temperature) and 200 μ L of a 0.41mM solution of
140 3,3',5,5'-Tetramethylbenzidine (TMB) (ref: 860336 from Sigma Aldrich) in 50mM
141 Na_2HPO_4 , 25mM citric acid and 0.0024% H_2O_2 , pH 5.5 solution was added to the plate
142 and incubated for 20 minutes at 37 °C. Finally, 50 μ L of a 1M sulfuric acid solution were
143 added and the absorbance was measured at 450nm with a plate reader (SpectroMax,
144 Molecular Device). For each sample, triplicates were performed and the fluorescence
145 value are the average of the 3 reads.

146

147 **Sequence alignment .**

148 Sequence alignment was done using Clustal Omega [46].

149

150 **Results and discussion**

151 SARS-CoV-2 is composed of 4 major structural proteins: S (spike), M (membrane), N
152 (nucleocapsid) and E (envelope) [47-49]. The spike protein is responsible for entry by
153 binding the angiotensin-converting enzyme 2 (ACE 2) on the host cell [50, 51].
154 Accordingly, antibodies that bind the RBD and inhibit the interaction of the S protein
155 with ACE 2 have been the center of attention. Based on the critical role of the S
156 protein in CoV infection, we focused our work on this protein, dissecting it into two
157 sets of overlapping linear 12mer peptides (two-fold sequence coverage with 6AA
158 overlap between the two sets; i.e 1-12, 7-18, 13-24,...). The peptide array was
159 prepared by hybridization of PNA-tagged peptide library onto a DNA microarray

160 (Figure 1) [52]. This technology insures a high level of homogeneity across different
161 arrays since individual arrays are prepared from the same library hybridized onto
162 commercial DNA microarrays. Furthermore, the arrays are designed to have each
163 sequence present 23 times, thus insuring high accuracy by calculating the median of
164 the observed fluorescence of the 23 spots.

165 The S protein of SARS-CoV-2 shares 76% homology with the SARS-CoV-1, [48, 53]
166 and this homology has already been harnessed to predict epitopes based on
167 experimental results from SARS-CoV-1. However, the different infection outcome of
168 SARS-CoV-2 relative to SARS-CoV-1 originates in part from differences in the S protein.
169 SARS-CoV-2 has better affinity to ACE 2 than SARS-CoV-1, yielding more efficient
170 cellular entry [54, 55]. Furthermore, the presence of a furin cleavage site [56-58] in
171 the S protein of SARS-CoV-2 (not present in SARS-CoV-1) coupled to an extended loop
172 at the proteolytic site leads to higher cleavage efficacy thus facilitating its activation
173 for membrane fusion [55, 59-61].

174 Analysis of 12 different plasma samples from SARS-CoV-2 infected patients and
175 comparison to 6 samples from uninfected patients clearly highlighted a strong
176 response to specific epitopes (Figure 2). The three linear epitopes most abundantly
177 detected (SARS-CoV-2 S protein) were: 655-672, 787-822, and 1147-1158. None of
178 these epitopes was singularly detected in all the positive samples tested, but each is
179 detected in >40% of the positive patients. The 655-672 epitope is the most detected in
180 positive samples and corresponds to a peptide that is not part of a secondary
181 structures (Fig 3A-B). The corresponding epitope had been also detected in SARS-CoV-
182 1 [8] (89% homology for the 18mer peptide, Fig 4A-C) and predicted bioinformatically
183 for SARS-CoV-2 [27, 31, 35, 36]; however, it had yet to be observed experimentally.

184 Interestingly, this epitope is just next to the reported S1/S2 cleavage site (Fig 4A-C,
185 furin/TMPRSS2) [50, 57]. The proteolytic cleavage of the loop 681-685 has been
186 demonstrated to be necessary for the viral entry into the host cell [50]. Moreover, the
187 proteolytic cleavage of the S protein could be a determinant factor for the capacity of
188 the virus to cross species. For example, the S protein of Uganda bats MERS-like CoV is
189 capable of binding human cells, but this is insufficient for entry [62]. However, if a
190 protease (trypsin) is added the protein is cleaved and viral entry occurs. Furthermore,
191 the most closely related virus to SARS-CoV-2 is RaTG-13 from a bat found in Yunnan
192 province in 2013 which does not contain the furin cleavage sequence [49]. Taken
193 together, this evidence suggest that cleavage of the S protein is a barrier to zoonotic
194 coronavirus transmission. Incorporation of the furin cleavage sites could have been
195 acquired by recombination with another virus leading to human infection. In relation
196 to the furin cleavage site, the pathogenic avian H5N1 contains such a furin cleavage
197 site that leads to higher pathogenicity due to the distribution of furins in multiple
198 tissues [63]. We speculate that the binding of an antibody to the epitope 655-672
199 would sterically block the proteolysis of S1/S2 and should thus be broadly neutralizing,
200 since the proteolysis is required for viral entry, without promoting ADE.

201 Another epitope abundantly detected only in healing patients was the 787-822, a
202 peptide segment extending at the periphery of the solvent exposed part of the protein
203 (Fig 3A-B). It has also been experimentally observed in the SARS-CoV-1 [9, 13], SARS-
204 CoV-2 [38, 39] and predicted bioinformatically [26, 27, 30, 31, 33, 36]. Interestingly,
205 this epitope includes the S2' cleavage site of the spike protein (Fig 4D-F), which has
206 been reported to activate the protein for membrane fusion via extensive irreversible
207 conformational changes [53, 64]. This epitope also includes the fusion peptide (816-

208 833, Fig 4D-F) [65] which is highly conserved among coronaviruses [66, 67], suggesting
209 a potential pan-coronavirus epitope at this location. It should be noted that a peptide-
210 based fusion inhibitor was shown to exhibit broad inhibitory activity across multiple
211 human CoVs [68] and that antibodies against that region have shown neutralizing
212 activity in SARS-CoV-1 [69]. Taken together, the data support the fact that antibodies
213 inhibiting this proteolytic cleavage should be neutralizing [61, 65].

214 Finally, the epitope 1147-1158 is found at the C terminus of the spike protein. The
215 structural data reported thus far did not suggest a defined structure for this portion of
216 the S protein. This epitope extends from the helix bundle 1140-1147 (Fig 3A-B) and had
217 also been experimentally observed in SARS-CoV-1 [9] and predicted bioinformatically
218 for SARS-CoV-2 [27, 31, 35].

219 One limitation of epitope mapping with a peptide array is that it is restricted to
220 linear epitopes. Antibodies binding to the RBD have been shown to participate in
221 interactions spanning multiple peptide fragments. Indeed, we did not observe a
222 strong response to linear peptides in the RBD. A control experiment with
223 AI334/CR3022 antibody [25, 70] showed only weak binding to 367-378 peptide
224 sequence of the RBD.

225 To validate the results observed on the microarray, a peptide (655-672) was
226 synthesized as a biotin conjugate for pull-down and ELISA experiments. The sequence
227 corresponding to 655-672-biotin and a scrambled version of the biotinylated peptide
228 were individually immobilized on agarose streptavidin beads. Beads were exposed to
229 serum from patients that were either positive or negative for that epitope based on
230 the microarray data and subsequently treated with anti-Human-IgG-FITC. The
231 fluorescence of the beads was quantified by confocal microscopy (Fig 5A). As can be

232 seen in Fig 5B-E, the beads with 655-672 peptide and positive serum sample showed
233 higher fluorescence than the ones with either negative serum or using the scrambled
234 peptide. To further probe the binding of 655-672 peptide to antibodies of SARS-CoV-2
235 positive patients, the same 655-672 biotinylated peptide was used in an ELISA assay
236 (Fig 6A). Three SARS-CoV-2 positive samples showing strong 655-672 signal (Samples
237 7, 8 and 9) and three SARS-CoV-2 negative samples (Samples 14, 15 and 17) were
238 analyzed showing clear binding to the 655-672 peptide and not to the scrambled
239 version (Fig 6B).

240 Next, an alanine scan was performed to assess the contribution of individual amino
241 acids to the interaction with the antibodies of two of the COVID positive patients
242 containing antibodies for this epitope (Sample number 1 and 6) at two different
243 dilutions (1 to 100 and 1 to 400). For this purpose, 17 different peptide-PNA
244 conjugates were synthesized, replacing one amino acid at the time with Ala (Fig 7A)
245 and measuring the intensity of the observed binding on the microarray. This analysis
246 revealed the key role of 5 residues that, if converted to Ala, lead to dramatic loss of
247 activity (amino acids in blue, Fig 7B). Thus, the key amino acids crucial for binding with
248 the antibodies common for these two plasma samples are H655, Y660, C662, G669 and
249 C671. The binding of the antibody presents in sample 1 also seems to depend on the
250 P665. The remarkable similarities between the two patients is notable considering a
251 polyclonal response.

252

253 **Conclusion**

254 We have developed a peptide array for the epitope mapping of the spike protein of
255 SARS-CoV-2. Using this array to profile healing plasma of twelve laboratory confirmed

256 COVID-19 patients and six negative controls we have discovered three
257 immunodominant linear regions, each present in >40% of COVID-19 patient. Two of
258 these epitopes correspond to key proteolytic sites on the spike protein (S1/S2 and the
259 S2') which have been shown to be crucial for viral entry and play an important role in
260 virus evolution and infection. The fact that antibodies binding to the protease
261 cleavage sites were identified from COVID-19 patients raises the possibility that other
262 mechanism than blocking the RBD-ACE2 interaction could be harnessed for
263 neutralization. Furthermore, blocking proteolytic cleavage could be important to
264 reduce antibody-dependent enhancement of viral entry, a key feature for vaccine
265 development. Full characterization of these antibodies is necessary, and efforts on this
266 direction are on their way.

267

268 **Acknowledgement**

269 The authors gratefully acknowledge funding from the University of Geneva and the
270 département d'instruction public du canton de Genève. The authors also gratefully
271 acknowledge Prof. Cosson from the Geneva Antibody Facility for generous gift of
272 reagents, and Isabelle Arm-Vernez from the virology laboratory of the laboratory
273 medicine division for the assessment of routine SARS-CoV-2 IgG serology.

274

275 **References**

- 276 1. Cohen J, Normile D. New SARS-like virus in China triggers alarm. *Science*.
277 2020;367(6475):234-5. Epub 2020/01/18. doi: 10.1126/science.367.6475.234. PubMed
278 PMID: 31949058.
- 279 2. Nicola M, Alsafi Z, Sohrabi C, Kerwan A, Al-Jabir A, Iosifidis C, et al. The socio-
280 economic implications of the coronavirus pandemic (COVID-19): A review.
281 *International Journal of Surgery*. 2020;78:185-93. doi:
282 <https://doi.org/10.1016/j.ijsu.2020.04.018>.

- 283 3. Jacob CO, Leitner M, Zamir A, Salomon D, Arnon R. Priming immunization
284 against cholera toxin and E. coli heat-labile toxin by a cholera toxin short peptide-beta-
285 galactosidase hybrid synthesized in E. coli. *EMBO J.* 1985;4(12):3339-43. Epub
286 1985/12/01. PubMed PMID: 3004953; PubMed Central PMCID: PMC554663.
- 287 4. Ahmad TA, Eweida AE, Sheweita SA. B-cell epitope mapping for the design of
288 vaccines and effective diagnostics. *Trials in Vaccinology.* 2016;5:71-83. doi:
289 <https://doi.org/10.1016/j.trivac.2016.04.003>.
- 290 5. Sawyer LA. Antibodies for the prevention and treatment of viral diseases.
291 *Antiviral Res.* 2000;47(2):57-77. Epub 2000/09/21. doi: 10.1016/s0166-3542(00)00111-
292 x. PubMed PMID: 10996394.
- 293 6. Babcock GJ, Eshaki DJ, Thomas WD, Jr., Ambrosino DM. Amino acids 270 to
294 510 of the severe acute respiratory syndrome coronavirus spike protein are required
295 for interaction with receptor. *J Virol.* 2004;78(9):4552-60. Epub 2004/04/14. doi:
296 10.1128/jvi.78.9.4552-4560.2004. PubMed PMID: 15078936; PubMed Central PMCID:
297 PMC387703.
- 298 7. Berry JD, Hay K, Rini JM, Yu M, Wang L, Plummer FA, et al. Neutralizing epitopes
299 of the SARS-CoV S-protein cluster independent of repertoire, antigen structure or mAb
300 technology. *MABs.* 2010;2(1):53-66. Epub 2010/02/20. doi: 10.4161/mabs.2.1.10788.
301 PubMed PMID: 20168090; PubMed Central PMCID: PMC2828578.
- 302 8. Guo JP, Petric M, Campbell W, McGeer PL. SARS corona virus peptides
303 recognized by antibodies in the sera of convalescent cases. *Virology.* 2004;324(2):251-
304 6. Epub 2004/06/23. doi: 10.1016/j.virol.2004.04.017. PubMed PMID: 15207612;
305 PubMed Central PMCID: PMC7125913.
- 306 9. He Y, Zhou Y, Wu H, Luo B, Chen J, Li W, et al. Identification of
307 immunodominant sites on the spike protein of severe acute respiratory syndrome
308 (SARS) coronavirus: implication for developing SARS diagnostics and vaccines. *J*
309 *Immunol.* 2004;173(6):4050-7. Epub 2004/09/10. doi: 10.4049/jimmunol.173.6.4050.
310 PubMed PMID: 15356154.
- 311 10. Zhou T, Wang H, Luo D, Rowe T, Wang Z, Hogan RJ, et al. An exposed domain in
312 the severe acute respiratory syndrome coronavirus spike protein induces neutralizing
313 antibodies. *J Virol.* 2004;78(13):7217-26. Epub 2004/06/15. doi:
314 10.1128/JVI.78.13.7217-7226.2004. PubMed PMID: 15194798; PubMed Central
315 PMCID: PMC421657.
- 316 11. Chou TH, Wang S, Sakhatskyy PV, Mboudjeka I, Lawrence JM, Huang S, et al.
317 Epitope mapping and biological function analysis of antibodies produced by
318 immunization of mice with an inactivated Chinese isolate of severe acute respiratory
319 syndrome-associated coronavirus (SARS-CoV). *Virology.* 2005;334(1):134-43. Epub
320 2005/03/08. doi: 10.1016/j.virol.2005.01.035. PubMed PMID: 15749129; PubMed
321 Central PMCID: PMC7111783.
- 322 12. van den Brink EN, Ter Meulen J, Cox F, Jongeneelen MA, Thijsse A, Throsby M,
323 et al. Molecular and biological characterization of human monoclonal antibodies
324 binding to the spike and nucleocapsid proteins of severe acute respiratory syndrome
325 coronavirus. *J Virol.* 2005;79(3):1635-44. Epub 2005/01/15. doi:
326 10.1128/JVI.79.3.1635-1644.2005. PubMed PMID: 15650189; PubMed Central PMCID:
327 PMC544131.
- 328 13. Zhong X, Yang H, Guo ZF, Sin WY, Chen W, Xu J, et al. B-cell responses in
329 patients who have recovered from severe acute respiratory syndrome target a

- 330 dominant site in the S2 domain of the surface spike glycoprotein. *J Virol.*
331 2005;79(6):3401-8. Epub 2005/02/26. doi: 10.1128/JVI.79.6.3401-3408.2005. PubMed
332 PMID: 15731234; PubMed Central PMCID: PMCPMC1075701.
- 333 14. Wang Q, Zhang L, Kuwahara K, Li L, Liu Z, Li T, et al. Immunodominant SARS
334 Coronavirus Epitopes in Humans Elicited both Enhancing and Neutralizing Effects on
335 Infection in Non-human Primates. *ACS Infect Dis.* 2016;2(5):361-76. Epub 2016/09/15.
336 doi: 10.1021/acsinfecdis.6b00006. PubMed PMID: 27627203; PubMed Central PMCID:
337 PMCPMC7075522.
- 338 15. Garber K. Coronavirus vaccine developers wary of errant antibodies. 2020. doi:
339 10.1038/d41587-020-00016-w.
- 340 16. Wan Y, Shang J, Sun S, Tai W, Chen J, Geng Q, et al. Molecular Mechanism for
341 Antibody-Dependent Enhancement of Coronavirus Entry. *J Virol.* 2020;94(5). Epub
342 2019/12/13. doi: 10.1128/JVI.02015-19. PubMed PMID: 31826992; PubMed Central
343 PMCID: PMCPMC7022351.
- 344 17. Graham BS. Rapid COVID-19 vaccine development. *Science.*
345 2020;368(6494):945-6. Epub 2020/05/10. doi: 10.1126/science.abb8923. PubMed
346 PMID: 32385100.
- 347 18. Pinto D, Park YJ, Beltramello M, Walls AC, Tortorici MA, Bianchi S, et al. Cross-
348 neutralization of SARS-CoV-2 by a human monoclonal SARS-CoV antibody. *Nature.*
349 2020. Epub 2020/05/19. doi: 10.1038/s41586-020-2349-y. PubMed PMID: 32422645.
- 350 19. Wang C, Li W, Drabek D, Okba NMA, van Haperen R, Osterhaus A, et al. A
351 human monoclonal antibody blocking SARS-CoV-2 infection. *Nat Commun.*
352 2020;11(1):2251. Epub 2020/05/06. doi: 10.1038/s41467-020-16256-y. PubMed PMID:
353 32366817; PubMed Central PMCID: PMCPMC7198537.
- 354 20. Cao Y, Su B, Guo X, Sun W, Deng Y, Bao L, et al. Potent neutralizing antibodies
355 against SARS-CoV-2 identified by high-throughput single-cell sequencing of
356 convalescent patients' B cells. *Cell.* 2020. Epub 2020/05/20. doi:
357 10.1016/j.cell.2020.05.025. PubMed PMID: 32425270; PubMed Central PMCID:
358 PMCPMC7231725.
- 359 21. Wu Y, Li C, Xia S, Tian X, Kong Y, Wang Z, et al. Identification of Human Single-
360 Domain Antibodies against SARS-CoV-2. *Cell Host Microbe.* 2020. Epub 2020/05/16.
361 doi: 10.1016/j.chom.2020.04.023. PubMed PMID: 32413276; PubMed Central PMCID:
362 PMCPMC7224157.
- 363 22. Seydoux E, Homad LJ, MacCamy AJ, Parks KR, Hurlburt NK, Jennewein MF, et al.
364 Characterization of neutralizing antibodies from a SARS-CoV-2 infected individual.
365 *bioRxiv.* 2020:2020.05.12.091298. doi: 10.1101/2020.05.12.091298.
- 366 23. Shi R, Shan C, Duan X, Chen Z, Liu P, Song J, et al. A human neutralizing antibody
367 targets the receptor binding site of SARS-CoV-2. *Nature.* 2020. Epub 2020/05/27. doi:
368 10.1038/s41586-020-2381-y. PubMed PMID: 32454512.
- 369 24. Wu Y, Wang F, Shen C, Peng W, Li D, Zhao C, et al. A noncompeting pair of
370 human neutralizing antibodies block COVID-19 virus binding to its receptor ACE2.
371 *Science.* 2020. Epub 2020/05/15. doi: 10.1126/science.abc2241. PubMed PMID:
372 32404477; PubMed Central PMCID: PMCPMC7223722.
- 373 25. Yuan M, Wu NC, Zhu X, Lee CD, So RTY, Lv H, et al. A highly conserved cryptic
374 epitope in the receptor-binding domains of SARS-CoV-2 and SARS-CoV. *Science.* 2020.
375 Epub 2020/04/05. doi: 10.1126/science.abb7269. PubMed PMID: 32245784; PubMed
376 Central PMCID: PMCPMC7164391.

- 377 26. Khan A, Alam A, Imam N, Siddiqui MF, Ishrat R. Design of an Epitope-Based
378 Peptide Vaccine against the Severe Acute Respiratory Syndrome Coronavirus-2 (SARS-
379 CoV-2): A Vaccine Informatics Approach. *bioRxiv*. 2020:2020.05.03.074930. doi:
380 10.1101/2020.05.03.074930.
- 381 27. Bhattacharya M, Sharma AR, Patra P, Ghosh P, Sharma G, Patra BC, et al.
382 Development of epitope-based peptide vaccine against novel coronavirus 2019 (SARS-
383 COV-2): Immunoinformatics approach. *J Med Virol*. 2020. Epub 2020/02/29. doi:
384 10.1002/jmv.25736. PubMed PMID: 32108359.
- 385 28. Mitra D, Shekhar N, Pandey J, Jain A, Swaroop S. Multi-epitope based peptide
386 vaccine design against SARS-CoV-2 using its spike protein. *bioRxiv*.
387 2020:2020.04.23.055467. doi: 10.1101/2020.04.23.055467.
- 388 29. Fast E, Chen B. Potential T-cell and B-cell Epitopes of 2019-nCoV. *bioRxiv*.
389 2020:2020.02.19.955484. doi: 10.1101/2020.02.19.955484.
- 390 30. Gao A, Chen Z, Segal FP, Carrington M, Streeck H, Chakraborty AK, et al.
391 Predicting the Immunogenicity of T cell epitopes: From HIV to SARS-CoV-2. *bioRxiv*.
392 2020:2020.05.14.095885. doi: 10.1101/2020.05.14.095885.
- 393 31. Parvez S, Preeti S. Prediction of T and B Cell Epitopes in the Proteome of SARS-
394 CoV-2 for Potential Use in Diagnostics and Vaccine Design 2020.
- 395 32. Li L, Sun T, He Y, Li W, Fan Y, Zhang J. Epitope-based peptide vaccine design and
396 target site characterization against novel coronavirus disease caused by SARS-CoV-2.
397 *bioRxiv*. 2020:2020.02.25.965434. doi: 10.1101/2020.02.25.965434.
- 398 33. Forcelloni S, Benedetti A, Dilucca M, Giansanti A. Identification of conserved
399 epitopes in SARS-CoV-2 spike and nucleocapsid protein. *bioRxiv*.
400 2020:2020.05.14.095133. doi: 10.1101/2020.05.14.095133.
- 401 34. Zheng M, Song L. Novel antibody epitopes dominate the antigenicity of spike
402 glycoprotein in SARS-CoV-2 compared to SARS-CoV. *Cell Mol Immunol*. 2020. Epub
403 2020/03/07. doi: 10.1038/s41423-020-0385-z. PubMed PMID: 32132669.
- 404 35. Ahmed SF, Quadeer AA, McKay MR. Preliminary Identification of Potential
405 Vaccine Targets for the COVID-19 Coronavirus (SARS-CoV-2) Based on SARS-CoV
406 Immunological Studies. *Viruses*. 2020;12(3). Epub 2020/02/29. doi:
407 10.3390/v12030254. PubMed PMID: 32106567; PubMed Central PMCID:
408 PMC7150947.
- 409 36. Grifoni A, Sidney J, Zhang Y, Scheuermann RH, Peters B, Sette A. A Sequence
410 Homology and Bioinformatic Approach Can Predict Candidate Targets for Immune
411 Responses to SARS-CoV-2. *Cell Host Microbe*. 2020;27(4):671-80 e2. Epub 2020/03/19.
412 doi: 10.1016/j.chom.2020.03.002. PubMed PMID: 32183941; PubMed Central PMCID:
413 PMC7142693.
- 414 37. Zhang B-z, Hu Y-f, Chen L-l, Tong Y-g, Hu J-c, Cai J-p, et al. Mapping the
415 Immunodominance Landscape of SARS-CoV-2 Spike Protein for the Design of Vaccines
416 against COVID-19. *bioRxiv*. 2020:2020.04.23.056853. doi: 10.1101/2020.04.23.056853.
- 417 38. Wang H, Hou X, Wu X, Liang T, Zhang X, Wang D, et al. SARS-CoV-2 proteome
418 microarray for mapping COVID-19 antibody interactions at amino acid resolution.
419 *bioRxiv*. 2020:2020.03.26.994756. doi: 10.1101/2020.03.26.994756.
- 420 39. Poh CM, Carissimo G, Wang B, Amrun SN, Lee CY-P, Chee RS-L, et al. Potent
421 neutralizing antibodies in the sera of convalescent COVID-19 patients are directed
422 against conserved linear epitopes on the SARS-CoV-2 spike protein. *bioRxiv*.
423 2020:2020.03.30.015461. doi: 10.1101/2020.03.30.015461.

- 424 40. Jegouic SM, Loureiro S, Thom M, Paliwal D, Jones IM. Recombinant SARS-CoV-2
425 spike proteins for sero-surveillance and epitope mapping. *bioRxiv*.
426 2020:2020.05.21.109298. doi: 10.1101/2020.05.21.109298.
- 427 41. Jiang H-w, Li Y, Zhang H-n, Wang W, Men D, Yang X, et al. Global profiling of
428 SARS-CoV-2 specific IgG/ IgM responses of convalescents using a proteome microarray.
429 *medRxiv*. 2020:2020.03.20.20039495. doi: 10.1101/2020.03.20.20039495.
- 430 42. Krishnamurthy HK, Jayaraman V, Krishna K, Rajasekaran KE, Wang T, Bei K, et al.
431 Antibody Profiling and Prevalence in the US population during the SARS-CoV2
432 Pandemic. *medRxiv*. 2020:2020.04.29.20085068. doi: 10.1101/2020.04.29.20085068.
- 433 43. Stringhini S, Wisniak A, Piumatti G, Azman AS, Lauer SA, Baysson H, et al.
434 Seroprevalence of anti-SARS-CoV-2 IgG antibodies in Geneva, Switzerland (SEROCoV-
435 POP): a population-based study. *The Lancet*. doi: 10.1016/S0140-6736(20)31304-0.
- 436 44. Zambaldo C, Barluenga S, Winssinger N. PNA-encoded chemical libraries. *Curr*
437 *Opin Chem Biol*. 2015;26:8-15. doi: 10.1016/j.cbpa.2015.01.005. PubMed PMID:
438 WOS:000357352400003.
- 439 45. Chouikhi D, Ciobanu M, Zambaldo C, Duplan V, Barluenga S, Winssinger N.
440 Expanding the Scope of PNA-Encoded Synthesis (PES): Mtt-Protected PNA Fully
441 Orthogonal to Fmoc Chemistry and a Broad Array of Robust Diversity-Generating
442 Reactions. *Chem-Eur J*. 2012;18(40):12698-704. doi: 10.1002/chem.201201337.
443 PubMed PMID: WOS:000309238400020.
- 444 46. Madeira F, Park YM, Lee J, Buso N, Gur T, Madhusoodanan N, et al. The EMBL-
445 EBI search and sequence analysis tools APIs in 2019. *Nucleic Acids Res*.
446 2019;47(W1):W636-W41. Epub 2019/04/13. doi: 10.1093/nar/gkz268. PubMed PMID:
447 30976793; PubMed Central PMCID: PMC6602479.
- 448 47. Wu F, Zhao S, Yu B, Chen YM, Wang W, Song ZG, et al. A new coronavirus
449 associated with human respiratory disease in China. *Nature*. 2020;579(7798):265-9.
450 Epub 2020/02/06. doi: 10.1038/s41586-020-2008-3. PubMed PMID: 32015508;
451 PubMed Central PMCID: PMC67094943.
- 452 48. Lu R, Zhao X, Li J, Niu P, Yang B, Wu H, et al. Genomic characterisation and
453 epidemiology of 2019 novel coronavirus: implications for virus origins and receptor
454 binding. *Lancet*. 2020;395(10224):565-74. Epub 2020/02/03. doi: 10.1016/S0140-
455 6736(20)30251-8. PubMed PMID: 32007145; PubMed Central PMCID:
456 PMC67159086.
- 457 49. Zhou P, Yang XL, Wang XG, Hu B, Zhang L, Zhang W, et al. A pneumonia
458 outbreak associated with a new coronavirus of probable bat origin. *Nature*.
459 2020;579(7798):270-3. Epub 2020/02/06. doi: 10.1038/s41586-020-2012-7. PubMed
460 PMID: 32015507; PubMed Central PMCID: PMC67095418.
- 461 50. Hoffmann M, Kleine-Weber H, Schroeder S, Kruger N, Herrler T, Erichsen S, et
462 al. SARS-CoV-2 Cell Entry Depends on ACE2 and TMPRSS2 and Is Blocked by a Clinically
463 Proven Protease Inhibitor. *Cell*. 2020;181(2):271-80 e8. Epub 2020/03/07. doi:
464 10.1016/j.cell.2020.02.052. PubMed PMID: 32142651; PubMed Central PMCID:
465 PMC67102627.
- 466 51. Yan R, Zhang Y, Li Y, Xia L, Guo Y, Zhou Q. Structural basis for the recognition of
467 SARS-CoV-2 by full-length human ACE2. *Science*. 2020;367(6485):1444-8. Epub
468 2020/03/07. doi: 10.1126/science.abb2762. PubMed PMID: 32132184; PubMed
469 Central PMCID: PMC67164635.

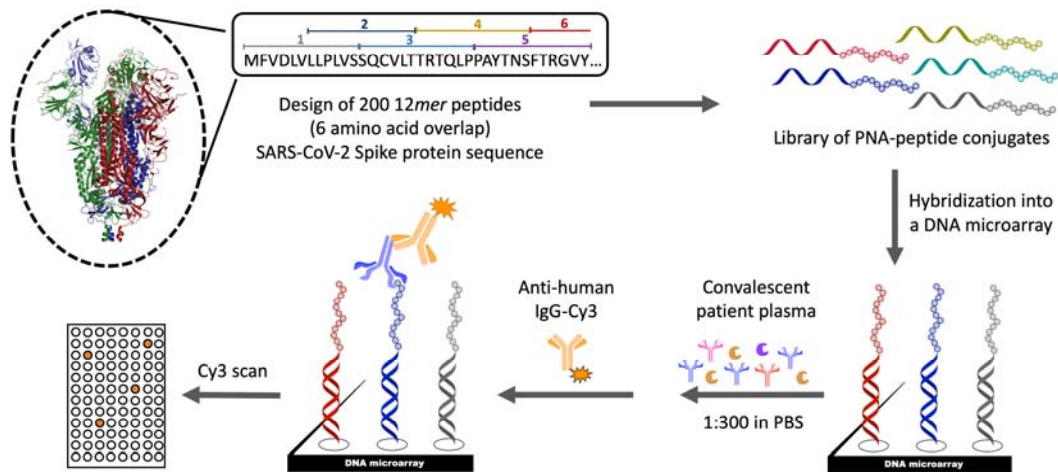
- 470 52. Harris JL, Winsinger N. PNA encoding (PNA = peptide nucleic acid): From
471 solution-based libraries to organized microarrays. *Chem-Eur J.* 2005;11(23):6792-801.
472 doi: 10.1002/chem.200500305. PubMed PMID: WOS:000233508800001.
- 473 53. Walls AC, Park YJ, Tortorici MA, Wall A, McGuire AT, Velesler D. Structure,
474 Function, and Antigenicity of the SARS-CoV-2 Spike Glycoprotein. *Cell.*
475 2020;181(2):281-92 e6. Epub 2020/03/11. doi: 10.1016/j.cell.2020.02.058. PubMed
476 PMID: 32155444; PubMed Central PMCID: PMC7102599.
- 477 54. Wrapp D, Wang N, Corbett KS, Goldsmith JA, Hsieh CL, Abiona O, et al. Cryo-EM
478 structure of the 2019-nCoV spike in the prefusion conformation. *Science.*
479 2020;367(6483):1260-3. Epub 2020/02/23. doi: 10.1126/science.abb2507. PubMed
480 PMID: 32075877; PubMed Central PMCID: PMC7164637.
- 481 55. Shang J, Wan Y, Luo C, Ye G, Geng Q, Auerbach A, et al. Cell entry mechanisms
482 of SARS-CoV-2. *Proc Natl Acad Sci U S A.* 2020;117(21):11727-34. Epub 2020/05/08.
483 doi: 10.1073/pnas.2003138117. PubMed PMID: 32376634; PubMed Central PMCID:
484 PMC7260975.
- 485 56. Cyranoski D. Profile of a killer virus. *Nature.* 2020;581:22-6.
- 486 57. Coutard B, Valle C, de Lamballerie X, Canard B, Seidah NG, Decroly E. The spike
487 glycoprotein of the new coronavirus 2019-nCoV contains a furin-like cleavage site
488 absent in CoV of the same clade. *Antiviral Res.* 2020;176:104742. Epub 2020/02/15.
489 doi: 10.1016/j.antiviral.2020.104742. PubMed PMID: 32057769; PubMed Central
490 PMCID: PMC7114094.
- 491 58. Wang Q, Qiu Y, Li JY, Zhou ZJ, Liao CH, Ge XY. A Unique Protease Cleavage Site
492 Predicted in the Spike Protein of the Novel Pneumonia Coronavirus (2019-nCoV)
493 Potentially Related to Viral Transmissibility. *Virology.* 2020. Epub 2020/03/22. doi:
494 10.1007/s12250-020-00212-7. PubMed PMID: 32198713; PubMed Central PMCID:
495 PMC7091172.
- 496 59. Meng T, Cao H, Zhang H, Kang Z, Xu D, Gong H, et al. The insert sequence in
497 SARS-CoV-2 enhances spike protein cleavage by TMPRSS. *bioRxiv.*
498 2020:2020.02.08.926006. doi: 10.1101/2020.02.08.926006.
- 499 60. Jaimes JA, Andre NM, Chappie JS, Millet JK, Whittaker GR. Phylogenetic Analysis
500 and Structural Modeling of SARS-CoV-2 Spike Protein Reveals an Evolutionary Distinct
501 and Proteolytically Sensitive Activation Loop. *J Mol Biol.* 2020;432(10):3309-25. Epub
502 2020/04/23. doi: 10.1016/j.jmb.2020.04.009. PubMed PMID: 32320687; PubMed
503 Central PMCID: PMC7166309.
- 504 61. Tang T, Bidon M, Jaimes JA, Whittaker GR, Daniel S. Coronavirus membrane
505 fusion mechanism offers a potential target for antiviral development. *Antiviral*
506 *Research.* 2020;178:104792. doi: <https://doi.org/10.1016/j.antiviral.2020.104792>.
- 507 62. Menachery VD, Dinno KH, 3rd, Yount BL, Jr., McAnarney ET, Gralinski LE, Hale
508 A, et al. Trypsin Treatment Unlocks Barrier for Zoonotic Bat Coronavirus Infection. *J*
509 *Virology.* 2020;94(5). Epub 2019/12/06. doi: 10.1128/JVI.01774-19. PubMed PMID:
510 31801868; PubMed Central PMCID: PMC7022341.
- 511 63. Luczo JM, Tachedjian M, Harper JA, Payne JS, Butler JM, Sapats SI, et al.
512 Evolution of high pathogenicity of H5 avian influenza virus: haemagglutinin cleavage
513 site selection of reverse-genetics mutants during passage in chickens. *Sci Rep.*
514 2018;8(1):11518. Epub 2018/08/03. doi: 10.1038/s41598-018-29944-z. PubMed PMID:
515 30068964; PubMed Central PMCID: PMC6070550.

- 516 64. Hoffmann M, Kleine-Weber H, Krüger N, Müller M, Drosten C, Pöhlmann S. The
517 novel coronavirus 2019 (2019-nCoV) uses the SARS-coronavirus receptor ACE2 and the
518 cellular protease TMPRSS2 for entry into target cells. bioRxiv.
519 2020:2020.01.31.929042. doi: 10.1101/2020.01.31.929042.
- 520 65. Zhu Y, Yu D, Yan H, Chong H, He Y. Design of potent membrane fusion inhibitors
521 against SARS-CoV-2, an emerging coronavirus with high fusogenic activity. bioRxiv.
522 2020:2020.03.26.009233. doi: 10.1101/2020.03.26.009233.
- 523 66. Madu IG, Roth SL, Belouzard S, Whittaker GR. Characterization of a highly
524 conserved domain within the severe acute respiratory syndrome coronavirus spike
525 protein S2 domain with characteristics of a viral fusion peptide. *J Virol*.
526 2009;83(15):7411-21. Epub 2009/05/15. doi: 10.1128/JVI.00079-09. PubMed PMID:
527 19439480; PubMed Central PMCID: PMC2708636.
- 528 67. Alsaadi EAJ, Neuman BW, Jones IM. A Fusion Peptide in the Spike Protein of
529 MERS Coronavirus. *Viruses*. 2019;11(9). Epub 2019/09/08. doi: 10.3390/v11090825.
530 PubMed PMID: 31491938; PubMed Central PMCID: PMC6784214.
- 531 68. Xia S, Yan L, Xu W, Agrawal AS, Algaissi A, Tseng CK, et al. A pan-coronavirus
532 fusion inhibitor targeting the HR1 domain of human coronavirus spike. *Sci Adv*.
533 2019;5(4):eaav4580. Epub 2019/04/17. doi: 10.1126/sciadv.aav4580. PubMed PMID:
534 30989115; PubMed Central PMCID: PMC6457931.
- 535 69. Miyoshi-Akiyama T, Ishida I, Fukushi M, Yamaguchi K, Matsuoka Y, Ishihara T, et
536 al. Fully human monoclonal antibody directed to proteolytic cleavage site in severe
537 acute respiratory syndrome (SARS) coronavirus S protein neutralizes the virus in a
538 rhesus macaque SARS model. *J Infect Dis*. 2011;203(11):1574-81. Epub 2011/05/20.
539 doi: 10.1093/infdis/jir084. PubMed PMID: 21592986; PubMed Central PMCID:
540 PMC7107252.
- 541 70. Hammel P, Marchetti A, Lima WC, Lau K, Pojer F, Hacker D, et al. AI334 and
542 AQ806 antibodies recognize the spike S protein from SARS-CoV-2 by ELISA. bioRxiv.
543 2020:2020.05.08.084103. doi: 10.1101/2020.05.08.084103.
- 544

545 **Supporting information**

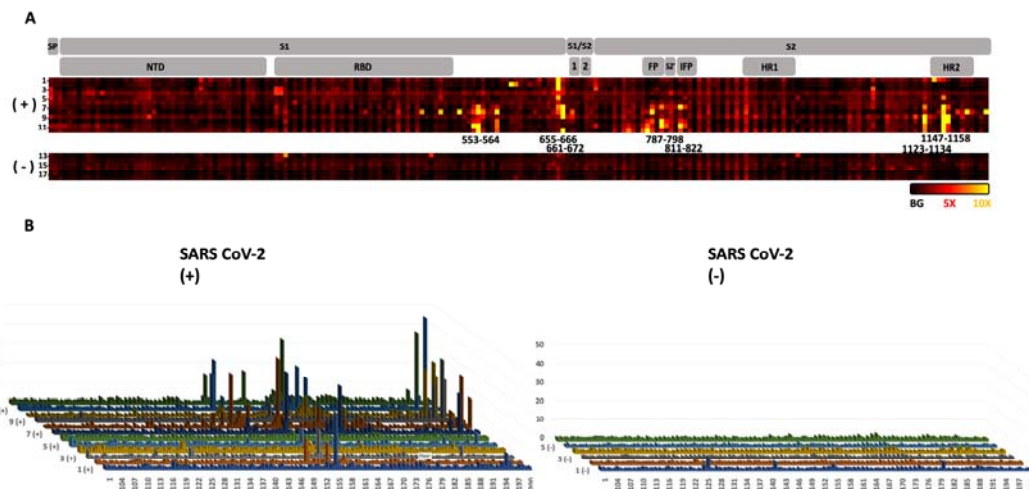
546 Detailed procedures and physical characterization of the synthetic products.

547



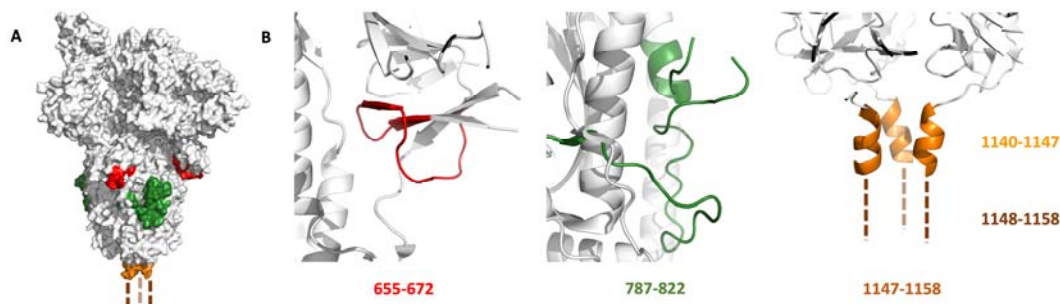
548
549
550
551
552

Fig 1. Schematic representation of the 200 membered Peptide-PNA epitope library design, DNA Microarray generation and experimental approach to map the antibody response of COVID-19 patients to the S protein of SARS-CoV-2.



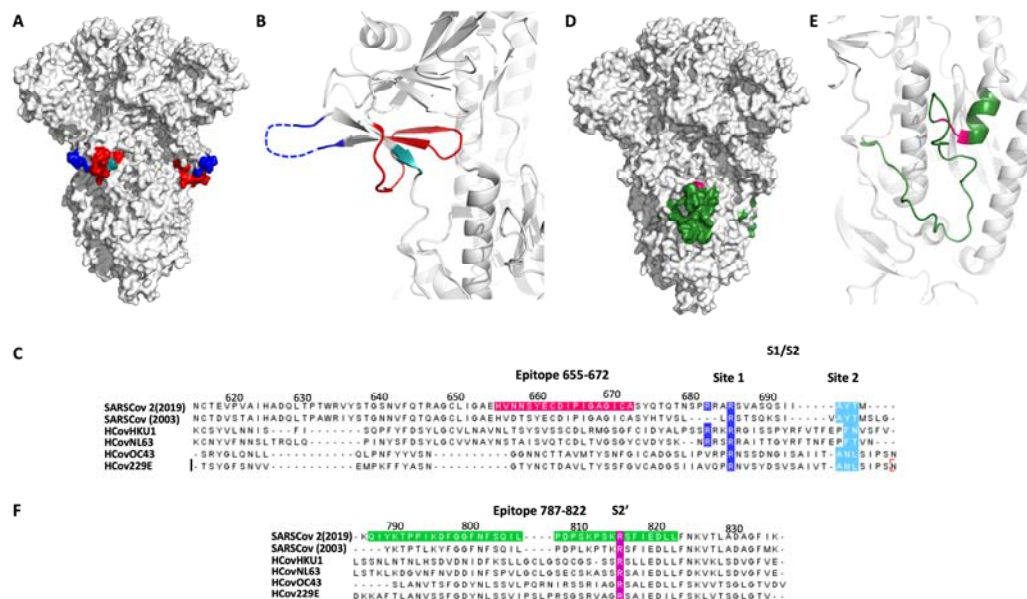
553
554
555
556
557
558
559
560
561
562
563
564
565
566
567
568
569

Fig 2. Antibody response from 12 convalescent SARS-CoV-2 patients and 6 uninfected negative controls. A: Domains of the spike protein (SP = Signal peptide, NTD = N-terminal domain, RBD = Receptor-binding domain, FP = Fusion Peptide, IFP = internal fusion protein, HR1 = Heptad repeat 1, HR2 = Heptad repeat 2) and heat map of antibody binding to the peptide fragments (black background intensity, red 5x background intensity and yellow 10x background intensity). Sample number are indicated on the left of the heat map. B: Fluorescence intensity of antibody binding from the 12 SARS-CoV-2 positive samples (left) and 6 SARS-CoV-2 negative samples (right). The fluorescence intensities are the median of 23 values followed by normalization to the background intensity. The immunodominant regions are highlighted with the corresponding residue numbers (the epitope numbers correspond to the column on top of the dash).



570
571
572
573
574
575

Fig 3. A) Localization of the three selected epitopes on the crystal structure of SARS-CoV-2 Spike protein (PDB ID: 6VYB): red (epitope 655-672), green (epitope 787-822) and orange (epitope 1147-1158, the structure is undefined in the PDB). B) Zoom of the 3 selected epitopes.

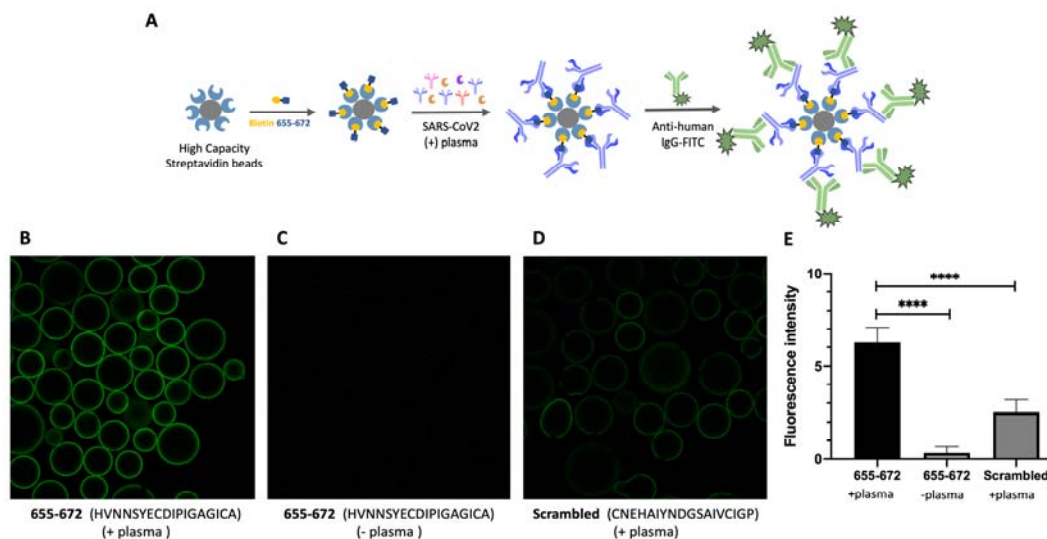


576

577

578 Fig 4. Selected epitopes localization in relation to the protease cleavage site of the
 579 spike protein. A-B) The 655-672 epitope (red) and the two reported protease cleavage
 580 sites S1/S2: site 1 (685-686: blue) and site 2 (695-696: cyan). C) Sequence alignment
 581 of the S1/S2 cleavage sites for five different coronaviruses SARSCov2(2019), SARSCov
 582 (2003), HCovHKU1, HCovNL63, HCOVOC43 and HCov229E. D-E) The 787-822 epitope
 583 (green) and the S2' cleavage site (815-816: magenta). F) Sequence alignment of the S2'
 584 cleavage site. Figure generated from pdb ID: 6VXX.

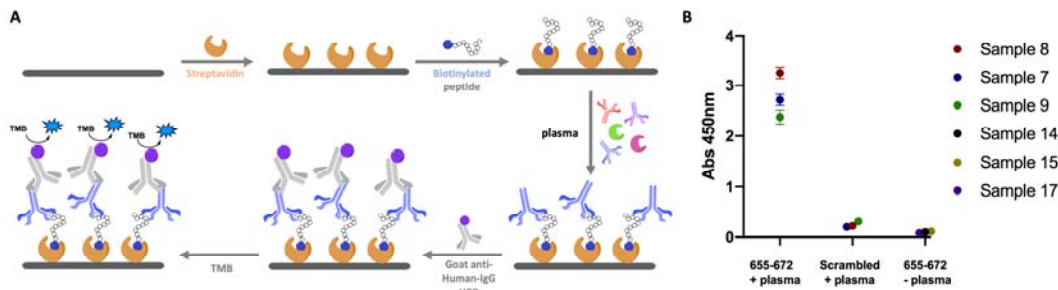
585



586

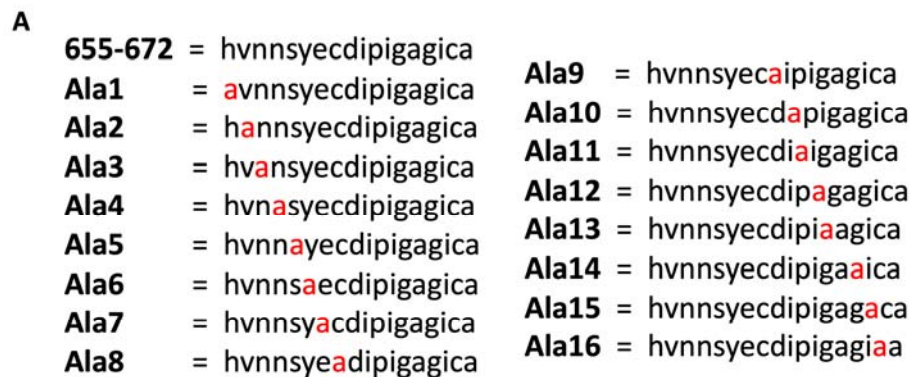
587

588 Fig 5. A) Schematic representation of epitope validation (anti-Spike-655-672 IgG in the
 589 SARS-CoV-2 positive patients' plasma). Microscope images of the beads with: B) Biotin
 590 655-672 with Positive plasma; C) Biotin 655-672 with Negative plasma; D) Biotin-
 591 scrambled peptide with Positive plasma. E) FITC fluorescence quantification of B, C and
 592 D.



593
594
595
596
597

Fig 6. A) Schematic representation of the ELISA assay. B) ELISA assay with 3 different 655-672 positive samples with the 655-672 peptide and scrambled peptide and 3 negative samples. Error bars represent triplicate experiments.



598
599
600
601
602
603
604
605

Fig 7. Alanine scan by hybridization of PNA-peptide conjugates Ala-1 to Ala-17 to a DNA microarray. A) Peptide sequences of the 17 PNA-peptide conjugates used for the alanine scan, where one amino acid at the time is modified by an alanine. B) Heat map of the interaction of 655-672 positive patient plasma with the different peptides-PNA conjugates hybridized in the DNA array at two different dilutions (1 to 100 and 1 to 400). Heat map represents the normalized fluoresce average of 23 different spots in the array.